Grinding-Induced Residual Stress Estimation by Indentation-Fracture Method in Ground Silicon Nitrides

Toshihiko Hoshide and Junko Abe

(Submitted 7 March 2001)

An estimating procedure for grinding-induced residual stress based on the indentation-fracture (IF) method was proposed by considering a nonuniform distribution of residual stress in the specimen depth. The proposed procedure was applied to gas pressure sintered and pressureless sintered silicon nitride ceramics, which were ground under different grinding conditions. The estimated residual stress was found to be compressive for both materials. The residual stress was dominantly affected by the grit size of the grinding wheel rather than the cutting depth. Although the dependency of the estimated residual stress on the grit size was different between the two materials, it was revealed that the estimated residual stress in both materials qualitatively corresponded with the stress measured by the x-ray diffraction method. In both materials, the bending strength was reasonably correlated with the estimated residual stress. It was elucidated that the proposed procedure was applicable to a relative evaluation of the grinding-induced residual stress in machined silicon nitride ceramics.

Keywords bending strength, grinding, indentation-fracture method, residual stress, silicon nitride

1. Introduction

Ceramic components, after their sintering processes, are usually machined to improve the accuracy of dimension in their engineering applications. Previous investigations[1–7] reveal that strength properties are influenced by grinding conditions. Particularly, it should be noted that residual stresses as well as surface flaws, which are generated in the grinding process of ceramics, may remarkably affect strength properties of ceramics. The x-ray stress measurement method is successfully used to estimate the residual stress in various materials. Considering practical needs, however, alternative simpler methods for the residual stress estimation are required even if they can give us only a relative estimation. For ceramics, especially, a possible candidate for the residual stress estimation is the indentation-fracture (IF) method,[5,8–11] which has been developed as a convenient procedure to evaluate the fracture toughness of ceramics. In the IF method, the length of an indentation-induced crack is one of dominant parameters in the fracture toughness evaluation, the crack length may be changed in a pre-existing residual stress field. This implies that the information on residual stress can be included in the toughness value evaluated by the IF method.

Previously, a uniform distribution of residual stress inside a ceramic material has been investigated by incorporating the residual stress into the stress intensity equilibrium of the crack induced by the IF method.[8–11] Experimental results, however, show that a distribution of residual stress due to grinding is macroscopically nonuniform toward the inside of a ceramic material.[4–6,12] Therefore, such a nonuniform distribution of residual stress should be adequately dealt with in the residual stress estimation based on the IF method.

In this work, an estimating procedure for grinding-induced residual stress is proposed by considering a nonuniform residual stress distribution in the IF method. Residual stresses in two kinds of silicon nitrides, which are machined under different grinding conditions, are estimated by using the proposed method. The estimated results are also discussed in comparison with residual stresses measured by the x-ray method and in correlation with strength properties.

Toshihiko Hoshide and **Junko Abe,** Department of Energy Conversion Science, Graduate School of Energy Science, Kyoto University, Sakyo-ku, Kyoto 606-8501, Japan. Contact e-mail: hoshide@energy.kyoto-u.ac.jp.

2. Principle of Estimating Residual Stress

2.1 Fracture Toughness Estimated by IF Method

Several formulae to evaluate the fracture toughness, K_C, of ceramics by using the IF method have been proposed (*e.g.*, Ref 13). For instance, the following equation based on the IF method is recommended in the Japanese Industrial Standard (JIS) R 1607.[14]

$$K_C = \frac{\alpha[EP]^{1/2}(d/2)}{a^{3/2}} \qquad \text{(Eq 1)}$$

where α, E, and P are an empirical coefficient, the Young's modulus of an indented material, and the indentation peak load set in a Vickers hardness tester, respectively. As illustrated in Fig. 1, other dimensions a and d are the half-surface length of a crack well developed after indentation and the diagonal length of a Vickers impression, respectively.

Other proposed formulae are basically similar to Eq 1; *i.e.*, they are constructed to be proportional to ($P^{1/2} \cdot a^{-3/2}$) and also include empirical coefficients, such as α in Eq 1. These coefficients are usually determined so that the residual stress associated with the indentation itself can be taken into account in the fracture toughness evaluation by the IF method. As for

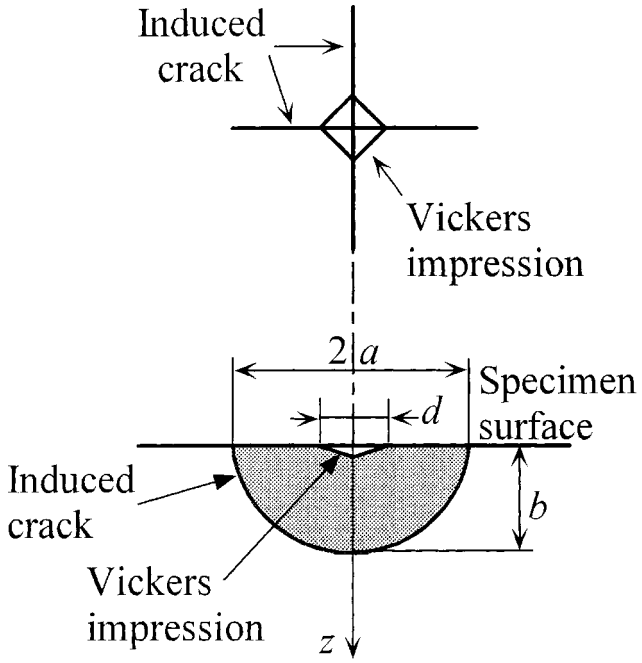

Fig. 1 Illustration of indentation-induced crack

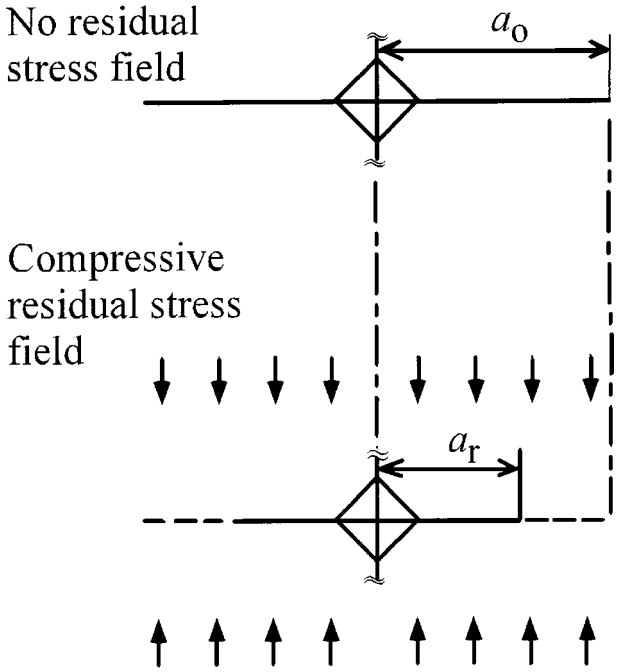

Fig. 2 Scheme of crack length variation due to compressive residual stress

the coefficient α in Eq 1, it has been empirically determined to be the mean value for several ceramic materials and is given as 0.026 for $2a/d$ larger than 2.5.[14] Since $2a/d$ may be smaller than 2.5 for some material/indentation-load systems, it is necessary to calibrate the α value for possible cases of $2a/d < 2.5$ by comparing K_C values calculated by Eq 1 with ones evaluated by the standard method using a single-edge precracked beam specimen method, which is primarily recommended in JIS R 1607 (or by other equivalent prcedures).

In the application of Eq 1, another point to note is that a slow crack growth (SCG) must not be caused by the residual stress field induced by an indentation. The SCG, to which oxide or glass ceramic materials especially are susceptible, leads to the time dependency of measured toughness.[11] The SCG effect on the toughness, however, is avoidable if the length of an indentation-induced crack is measured as soon as possible after the indentation.

2.2 Critical Equilibrium Condition in Indented Material with Residual Stress

Equation 1 can be applied to materials free of pre-existing stresses. At a critical level for equilibrium crack growth in an indented ceramic material with a residual stress, the net stress intensity factor, K_{net}, remains constant:[9]

$$K_{\text{net}} = K_{CA} + K_R = K_C \qquad \text{(Eq 2)}$$

In Eq 2, K_{CA} is an apparent fracture toughness affected by the residual stress, and K_R is a residual stress intensity factor associated with the residual stress field. The stress intensity parameters, K_{CA} and K_R, are evaluated as follows.

Evaluation of Apparent Fracture Toughness. If a material has a compressive stress, which often appears in ground ceramics, as illustrated in Fig. 2, the crack length, a_r, in the indented material becomes shorter compared with the crack length, a_o, in the same material but free of pre-existing stresses, even under an identical indentation load, P_o. In a material without any residual stress, Eq 1 gives

$$K_C = \frac{\alpha[EP_o]^{1/2}(d/2)}{a_o^{3/2}} \qquad \text{(Eq 3)}$$

For a material with a residual stress, the fracture toughness K_{CA} is evaluated by applying a measured crack length a_r instead of a_o in Eq 3 as

$$K_{CA} = \frac{\alpha[EP_o]^{1/2}(d/2)}{a_r^{3/2}} \qquad \text{(Eq 4)}$$

Equation 4 should be interpreted as an apparent fracture toughness. In the above cases, it is empirically known that the diagonal length, d, for the same indentation load is not so much affected by the grinding-induced residual stress.[5] Therefore, the identical value of d may be applicable to both Eq 3 and 4 irrespective of the residual stress.

Evaluation of Residual Stress Intensity Factor. A grinding-induced residual stress, σ_R, is generally known to be compressive. In experimental studies,[4–6,12] it is also reported that the compressive residual stress, σ_R, has its peak, σ_{RO}, on or near the ground surface of a specimen and vanishes toward the specimen-depth direction, *i.e.*, the z direction in Fig. 1. Such a nonuniform distribution of residual stress in the depth direction should be taken into account in evaluating the residual stress intensity factor.

Consider a crack system subjected to a residual stress, σ_R, given by

$$\sigma_R = \sigma_{RO} f(z) \quad \text{(Eq 5)}$$

where $f(z)$ is a function of z to specify the residual stress distribution in the z direction. Since a well-developed crack induced by the indentation is approximated as a semielliptical crack, K_R, for the crack subjected to the residual stress given by Eq 5 is usually expressed as the following form:

$$K_R = \frac{\sigma_{RO}(\pi\lambda a)^{1/2}}{\Phi(\lambda)} M_R \quad \text{(Eq 6)}$$

In Eq 6, λ is the aspect ratio defined as the ratio b/a of the crack depth, b, to the surface half-length, a, and $\Phi(\lambda)$ is the complete elliptic integral of the second type depending on λ. The parameter M_R in Eq 6 is a magnification factor, which is determined by the residual stress distribution, $f(z)$, in Eq 5, λ and b/t, where t is the specimen thickness.

2.3 Residual Stress Estimate by IF Method

By substituting Eq 4 and 6 with a_r into Eq 2, we obtain the following equation to estimate the peak residual stress, σ_{RO}.

$$\sigma_{RO} = \frac{K_C - \alpha(EP_o)^{1/2}(d/2)(a_r)^{-3/2}}{(\pi\lambda)^{1/2}(a_r)^{1/2} M_R} \Phi(\lambda) \quad \text{(Eq 7)}$$

If it is assumed that the crack is closed to change its length from a_o to a_r ($<a_o$) by the compressive residual stress, the residual stress intensity, K_R, associated with the residual stress is evaluated by using a_o for a in Eq 6. In this case, another estimation for the peak residual stress must be expressed as follows.

$$\sigma_{RO} = \frac{K_C - \alpha(EP_o)^{1/2}(d/2)(a_r)^{-3/2}}{(\pi\lambda)^{1/2}(a_o)^{1/2} M_R} \Phi(\lambda) \quad \text{(Eq 8)}$$

In applying Eq 8, $(a_o)^{1/2}$ may be calculated from Eq 3 as

$$(a_o)^{1/2} = \left[\frac{\alpha(EP_o)^{1/2} d}{2K_C}\right]^{1/3} \quad \text{(Eq 9)}$$

where all parameters on the right-hand side are known or given.

3. Experiments

3.1 Materials

Materials to be used have been investigated in other works, *i.e.*, a gas pressure sintered silicon nitride produced by NGK Spark Plug Co. Ltd.[15] and a pressureless sintered silicon nitride by TOTO Ltd.[5] In the following, the pressure sintered and the pressureless sintered silicon nitrides are designated SN-GP and SN-PL, respectively. The bulk density, ρ, the Young's modulus, E, and the fracture toughness, K_C, of the materials are as follows: ρ = 3.23 Mg/m^3, E = 320 GPa, and K_C = 6.0 MPa $\cdot \sqrt{\text{m}}$ for SN-GP; and ρ = 3.23 Mg/m^3, E = 310 GPa, and K_C = 5.7 MPa $\cdot \sqrt{\text{m}}$ for SN-PL. The fracture toughness of each material was obtained by the standard method specified in JIS R 1607 or its equivalent procedure.

3.2 Specimen Preparations

The geometry of the specimen machined in this work was of a square rod type with a dimension of 4 × 3 × 36 mm, which is specified for the standard bending specimen in JIS R 1601.[16] In all cases, the grinding direction was set in the longitudinal direction of the specimen.

For SN-GP, two series of specimens were finally prepared by grinding with wheels of #400 and #800 grit sizes. The cutting depth per one pass was set to be 4 μm for #400 grinding and 2 μm for #800 grinding, respectively. Before the final grinding, all specimens of SN-GP had been ground by using #400 grit wheels.

On the other hand, specimens of SN-PL were machined under six different conditions as follows. Three distinct grit sizes of grinding wheel, #170, #270, and #600, were adopted. Two values of the cutting depth were selected for each grit size; *i.e.*, 5 and 40 μm for #170 and #270, and 1 and 25 μm for #600. All specimens had been machined using #400 grit wheels before the final grinding, as stated previously.

Combining respective digits of the grit size and the cutting depth, materials ground under the aforementioned conditions are designated 400-04 and 800-02 for SN-GP, and 170-05, 170-40, 270-05, 270-40, 600-01, and 600-25 for SN-PL. For instance, 170-05 represents the material ground by 5 μm using a wheel with grit size of #170.

3.3 Indentation Procedures and Indentation-Induced Cracks

In the present study, specimens were indented by using an ordinary Vickers hardness tester. The distance between the centers of adjacent indents was kept longer than 10a, where a is the half-surface length of an indentation-induced crack.

The surface length, 2a, of the crack was measured through an optical microscope, while the crack tip was sometimes identified by using a laser scanning microscope with a higher resolving power. The crack depth, b, was measured by polishing the surface of a cracked specimen until the crack disappeared on the polished surface. The aspect ratio of the indentation-induced crack was calculated as b/a by using measured values. It was observed that the mean aspect ratio was 1 for SN-GP and 0.55 for SN-PL.

3.4 Calibration of Coefficient α with Respect to 2a/d

As mentioned previously, the length, a, of the indentation-induced crack is supposed to change due to the residual stress generated by grinding, though the diagonal length, d, of the Vickers impression is hardly affected by the grinding-induced residual stress. This implies that the ratio $2a/d$ may change according to the variation in residual stress. To investigate the above subject, SN-GP materials free of residual stress were prepared by annealing after polishing their ground surfaces.

Using the prepared materials, several values of $2a/d$ expected

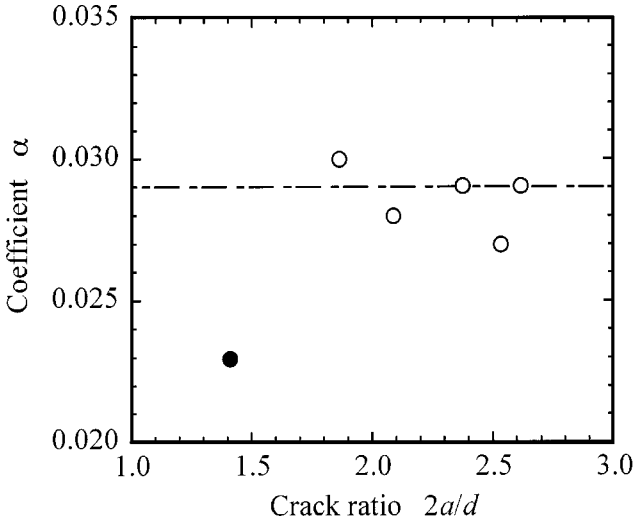

Fig. 3 Variation of coefficient in toughness evaluation based on the IF method with respect to crack ratio

in experiments were obtained by changing the indentation load. The resultant range was of $2a/d$ from 1.4 to 2.5. The α value in Eq 1 was calibrated for these values of $2a/d$ by comparing the K_C value evaluated by Eq 1 with that evaluated by the JIS standard method or its equivalent procedure. In Fig. 3, the α value is plotted with respect to $2a/d$. The α value is found to be almost constant in the examined region except for a range of $2a/d$ less than 1.6. The constant α value in the range of $2a/d$ from 1.8 to 2.5, however, was sufficient in the regime to be investigated. The dot-dashed line in Fig. 3 indicates the mean 0.029 of α values for other silicon nitrides shown in JIS R 1607. As seen in Fig. 3, the present results in the $2a/d$ region larger than 1.8 almost coincide with the reference data, which will be used in the following analysis. It should be noted that 0.029 for silicon nitrides is different from the average value of 0.026 for three kinds of ceramics; *i.e.*, alumina with $\alpha = 0.027$, silicon carbide with $\alpha = 0.023$, and silicon nitride with $\alpha = 0.029$ in JIS R 1607.

4. Application of IF Method to Residual Stress Estimation in Silicon Nitrides

It is experimentally observed that the compressive residual stress caused by grinding vanishes at the depth of 20 to 30 μm from the ground surface in several silicon nitrides.[6–8] This suggests that the grinding-induced residual stress sharply vanishes toward the specimen depth or changes its sign near the ground specimen surface. Unfortunately, an actual distribution of residual stress, $f(z)$ in Eq 5, is unknown in most cases. Consequently, in this analysis, $f(z)$ is presumed to be approximated by the following cubic function of z as one of the simple functions, which steeply decreases with respect to z.

$$f(z) = (1 - z/b)^3 \qquad \text{(Eq 10)}$$

By using Eq 10, it is also postulated that the residual stress acts within the region from the surface to the crack depth, b; *i.e.*, $0 \le z/b \le 1$. An advantage in the application of the stress distribution (Eq 10) is that numerical data of magnification factors, M_R in Eq 6, are available elsewhere.[17] This is very convenient for the actual usage of the present procedure.

Now, the peak residual stress, σ_{RO}, for each case can be estimated by using Eq 7 for the assumed stress distribution of Eq 10. Table 1 shows the mean and the coefficient of variation of the residual stress, σ_{RO}, estimated by using several specimens for each case. When Eq 8 instead of Eq 7 is applied to the estimation, it is found that the estimated values are reduced by 10 to 20% compared with the results in Table 1. In SN-GP materials, it is seen that grinding with a rougher wheel, *i.e.*, a smaller mesh size, results in a smaller compressive residual stress. As for SN-PL, however, a material ground using a rougher wheel is found to have a larger compressive residual stress, though the residual stress is hardly affected by the cutting depth. It is supposed that the difference in the dependence on the wheel grit size between the two materials is associated with discrepancies in more detailed grinding conditions specified by other factors, such as down or upper cut, cross feeding, table speed, wheel speed, use of lubricants and coolants, number of spark-outs, *etc.*

5. Discussion

5.1 Comparison of Estimation by IF Method with X-Ray Measurements

Residual stress measurements by the x-ray diffraction method have been done for the SN-GP materials ground under the same conditions.[18] The mean and the coefficient of variation of measured residual stresses are −26.1 MPa and 0.269 for 400-04, and −43.4 MPa and 0.209 for 800-02. For this material/grinding system, it is found that a smaller compressive residual stress is measured for a more roughly ground material. This tendency qualitatively coincides with the peak residual stress, σ_{RO}, estimated by the proposed procedure, though the procedure gives an overestimate of compressive stress.

On the other hand, no measurement by x-ray is available for the same material system as SN-PL. Therefore, the measurement by the x-ray method for a similar material, *i.e.*, another pressureless sintered silicon nitride,[4] is cited here as reference data. The data reveal that the mean and the coefficient of variation of residual stress are −541 MPa and 0.0538 in the material ground using a #80 mesh wheel, and −192 MPa and 0.0677 in the material ground using a #200 mesh wheel. The peak value, σ_{RO}, around −450 MPa, which is estimated for the 170-system materials, exists between the values for the materials ground by using #80 and #200 grit wheels, though the estimated value is closer to the x-ray measurement for the material ground by an #80 mesh wheel. The previous x-ray measurement also implies that grinding with a rougher wheel brings about a larger compressive stress. This trend qualitatively coincides with the results in SN-PL, as shown in Table 1.

The aforementioned x-ray results in both materials represent similar trends, which are seen in the estimates by the proposed procedure. Consequently, it may be concluded that the proposed

Table 1 Surface residual stress estimated by the IF method

Material	SN-GP		SN-PL					
Identification	**400-04**	**800-02**	**170-05**	**170-40**	**270-05**	**270-40**	**600-01**	**600-25**
Residual stress σ_{RO} (MPa)	−243	−359	−464	−440	−309	−242	−197	−198
Coefficient of variation	0.150	0.121	0.110	0.0505	0.168	0.229	0.0909	0.337

Table 2 Residual stress averaged in specimen-depth direction

Material	SN-GP		SN-PL					
Identification	**400-04**	**800-02**	**170-05**	**170-40**	**270-05**	**270-40**	**600-01**	**600-25**
Residual stress $\sigma_{R,\text{ave}}$ (MPa)	−60.9	−89.8	−116	−110	−77.1	−60.6	−49.3	−49.4

Table 3 Statistics of bending strength in silicon nitride ceramics

Material	SN-GP(a)		SN-PL(b)					
Identification	**400-04**	**800-02**	**170-05**	**170-40**	**270-05**	**270-40**	**600-01**	**600-25**
Mean strength σ_f (MPa)	1010	1070	961	952	930	933	896	921
Coefficient of variation	0.0620	0.0736	0.0446	0.0512	0.0775	0.0641	0.0785	0.0527

(a) Four-point bending tests
(b) Three-point bending tests

procedure gives a qualitative correspondence to the x-ray measurement. This implies that the proposed procedure is applicable to a relative estimation of grinding induced residual stress.

5.2 Discussion of Comparison between Residual Stresses Evaluated by X-Ray and IF Methods

In quantitatively comparing the residual stress estimates by the IF method with the x-ray measurements, it should be noted that the x-ray penetrates into a material in the x-ray diffraction method. This means that the stress averaged within the penetration depth, z_p, of x-ray into the material from the surface is measured by the x-ray method. Therefore, the estimated residual stress should be averaged in the depth, z_p, in comparison with x-ray measurements. In the present procedure, the averaged residual stress, $\sigma_{R,\text{ave}}$ may be evaluated by

$$\sigma_{R,\text{ave}} = \frac{\sigma_{RO}}{z_p} \int_0^{z_p} f(z)\, dz. \qquad \text{(Eq 11)}$$

Unfortunately, the depth, z_p, is not clear for an arbitrary material/x-ray diffraction system. By way of trial, the residual stress with the distribution expressed by Eq 10 is averaged in the region of $0 \leq z \leq b$. This trial implies that z_p in Eq 11 is replaced with b. The calculated residual stress, $\sigma_{R,\text{ave}}$, is listed in Table 2. It is found that the averaged residual stress, $\sigma_{R,\text{ave}}$, in SN-GP is reduced to the value measured by the x-ray method. Contrary to the trend observed in the estimated peak residual stress, σ_{RO}, the calculated $\sigma_{R,\text{ave}}$ of about −110 MPa for the 170-system materials of SN-PL is closer to the x-ray measurement of −192 MPa for the other pressureless sintered silicon nitride ground by a #200 mesh wheel rather than that measured in the material ground using an #80 mesh wheel.

5.3 Relation between Strength and Estimated Residual Stress

As mentioned in Section 1, the strength of ceramic materials is affected by the residual stress. In this section, the strength is correlated with the grinding-induced residual stress estimated by the proposed procedure.

Bending strength has been obtained for SN-GP[15] and SN-PL,[5] respectively. Smooth specimens of SN-GP were loaded by four-point bending with an outer span of 30 mm and an inner span of 10 mm, while bending tests for smooth specimens of SN-PL were conducted under three-point mode with a span length of 20 mm. In both cases, tests were carried out under load-controlled condition, and the loading rate was controlled so that the rate of the maximum tensile stress in a specimen might be about 100 MPa/s. Statistics of bending strength for each material are summarized in Table 3.

In Fig. 4, the mean strength, σ_f, depending on the grinding condition, is correlated with the peak residual stress, σ_{RO}, estimated previously. For both materials, a larger compressive residual stress is found to result in a larger strength. Of course, a similar trend is also seen when the averaged residual stress, $\sigma_{R,\text{ave}}$, instead of the peak one is correlated with the strength. It is concluded that the result shown in Fig. 4 is reasonable, because the compressive stress restrains the crack growth from inherent flaws and improves the material strength.

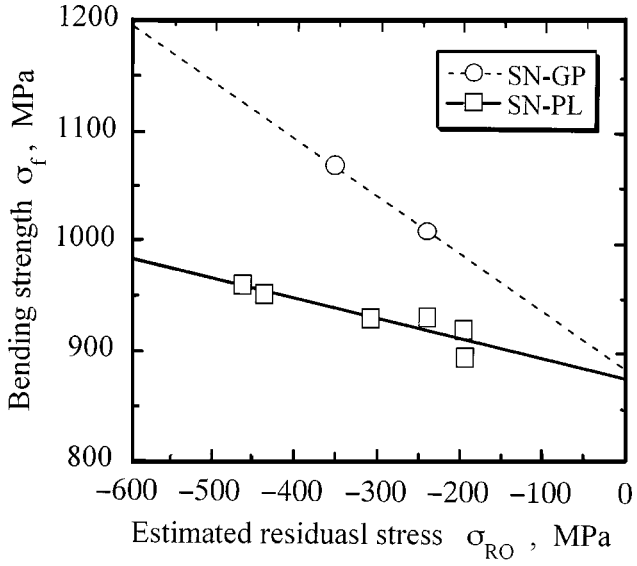

Fig. 4 Relation between estimated residual stress and bending strength

6. Concluding Remarks

In this work, an estimation of grinding-induced residual stress by using the indentation-fracture method was presented for materials that had nonuniform residual stress distributions in the specimen-depth direction. The residual stress distribution was assumed as the cubic function of the depth from a specimen surface. The proposed procedure was applied to gas pressure sintered and pressureless sintered silicon nitrides, which were ground under different grinding conditions. It was revealed that estimated residual stresses were compressive for both materials. The grit size of the grinding wheel dominantly affected the residual stress. Although the dependency of the estimated residual stress on the grit size was different between the two materials, it was clarified that the estimated residual stress qualitatively coincided with the stress measured by the x-ray diffraction method in respective materials. A reasonable correlation was also seen between the estimated residual stress and the bending strength; *i.e.*, a larger compressive residual stress increased the strength. Consequently, it was concluded that the proposed procedure was effective in a qualitative estimation of grinding-induced residual stress.

Finally, it should be remarked that some restrictions on the application of the present procedure are imposed in practice. The application requires *a priori* information on the distribution form of residual stress in the specimen-depth direction as well as the aspect ratio of an indentation-induced crack, which may be influenced by the residual stress state.

Acknowledgment

The authors are indebted to Mr. N. Masago, a graduate student of Kyoto University, for his cooperation in a part of experiments.

References

1. D. Lewis III: *Ceram. Bull.*, 1982, vol. 61 (11), pp. 1208-14.
2. H. Fessler, D.C. Fricker, and D.J. Godfrey: *Ceram.-Perform. Appl.*, 1983, vol. 3, pp. 705-36.
3. M.W. Hawmann, P.H. Cohen, J.C. Conway, and R.N. Pangborn: *J. Mater. Sci.*, 1985, vol. 20, pp. 482-90.
4. K. Tanaka, K. Suzuki, and Y. Yamamoto: *Proc. Int. Conf. Residual Stresses*, G. Beck, S. Denis, and A. Simon, eds., Elsevier Applied Science, New York, NY, 1989, pp. 15-26.
5. T. Hoshide, K. Okumura, and T. Inoue: *J. Soc. Mater. Sci., Jpn.*, 1991, vol. 40 (449), pp. 217-33.
6. K. Suzuki and K. Tanaka: *J. Soc. Mater. Sci., Jpn.*, 1991, vol. 40 (454), pp. 818-24.
7. D.W. Richerson: *Modern Ceramic Engineering Properties, Processing, and Use in Design*, Marcel Dekker, Inc., New York, NY, 1992.
8. D.B. Marshall and B.R. Lawn: *J. Mater. Sci.*, 1979, vol. 14, pp. 2001-12.
9. D.B. Marshall, B.R. Lawn, and P. Chantikul: *J. Mater. Sci.*, 1979, vol. 14, pp. 2225-35.
10. K. Zeng and D. Rowcliffe: "Experimental Measurement of Residual Stress Field around a Sharp Indentation in Glass," Paper No. SIX-23-93, Apr. 1993, American Ceramic Society, Cincinnati, OH.
11. J. Salomonson and D. Rowcliffe: *J. Am. Ceram. Soc.*, 1995, vol. 78 (1), pp. 173-77.
12. Y. Sakaida, S. Harada, and K. Tanaka: *J. Soc. Mater. Sci., Jpn.*, 1993, vol. 42 (477), pp. 641-47.
13. B.R. Lawn: in *Fracture Mechanics of Ceramics*, R.C. Bradt, A.G. Evans, D.P.H. Hasselman, and F.F. Lange, eds., Plenum Press, New York, NY, 1983.
14. "Testing Methods for Flexural Strength (Modulus of Rupture) of High Performance Ceramics," Japanese Industrial Standard JIS R 1607, Japanese Standards Association, Tokyo, 1995.
15. T. Hoshide and M. Masuda: *Mater. Sci. Res. Int.*, 1995, vol. 1 (2), pp. 108-13.
16. "Testing Methods for Fracture Toughness of High Performance Ceramics," Japanese Industrial Standard JIS R 1601, Japanese Standards Association, Tokyo, 1990.
17. *Stress Intensity Factors Handbook*, Y. Murakami, S. Aoki, N. Hasebe, Y. Itoh, H. Miyata, N. Miyazaki, H. Terada, K. Togho, M. Toya, and R. Yuuki, eds., Pergamon Press, Oxford, United Kingdom, 1987.
18. S. Harada: Report No. 98-A-419, Japan Fine Ceramics Center, Nagoya, Jan. 1999.